Journal of Air-Conditioning and Refrigertion Volume 7 September (1999) / pp. 101~111

An Experimental Study on the Defrosting Behavior of a Fin-Tube Heat Exchanger

Kwan Soo Lee* and Sung Jhee**

Key Words : Defrost, Fin-tube heat exchanger, Electric heater, Defrosting efficiency, Melting efficiency

Abstract

The effect of various conditions of frosting and defrosting on the defrosting behavior of a fin-tube heat exchanger has been examined experimentally. An electric heater is used for defrosting in a fin-tube heat exchanger. There are several local maxima in the water draining rate. The amount of residual water on the heat exchanger after completion of defrosting is kept constant due to surface tension on the heat exchanger. Without considering degradation of the thermal performance due to the frosting, the defrosting efficiency is improved with increasing amount of frost irrespective of the frosting condition. The defrosting behavior is affected by frosting density as well as frost accumulation, both of which vary with the experimental operating conditions. The heat loss to the surrounding air decreases, and melting and defrosting efficiencies show high values with decreasing heat input.

Nomenclature

L : Latent heat of sublimation, [J/g]

Mw : Accumulation weight of draining water, [g]

Mw,res : Weight of residual water, [g]

mf : Frost mass, [g]

qheater : Power supply for defrosting, [W]

T : Temperature, [℃]

t : Time, [min]

tp : Melting preparation period, [min]

tm : Frost melting period, [min]

tr : Moisture removal period, [min]

* Member of SAREK, School of Mechanical Engineering, Hanyang University, Haengdang-dong, Sungdong-ku, Seoul, 133-791, Korea

** Member of SAREK, Graduate Assistant in the Department of Mechanical Engineering, Hanyang University, Haengdang-dong, Sungdong-ku, Seoul, 133-791, Korea

trest : Rest period, [min]
$\dot{w}$: Water draining rate, [g/s]
$\dot{w}$rest : Water draining rate at rest period, [g/s]

Greek Symbols

ηd : Defrosting efficiency, [%]
ηm : Melting efficiency, [%]
τd : Defrosting time, [min]
τm : Melting time, [min]

1. Introduction

Frost forms on the cooling surface of a low temperature heat exchanger when water vapor in the surrounding air adheres to the cooling surface via simultaneous heat and mass transfer. The frost reduces the heat transfer rate, and also degrades the performance of the refrigeration system by reducing the air flow area inside the heat exchanger. Therefore, in order to maintain the proper performance of the heat exchanger, defrosting should be activated periodically to remove such frost. However, the entire refrigeration system has to be paused when defrosting is active, and excessive defrosting heat supplied to the system degrades performance as well. Hence, both frosting and defrosting degrade the refrigeration system performance.

Despite the importance of defrosting, most of the focus has been on understanding the general phenomena during frosting process.[1-6] Only few previous studies on defrosting have been conducted, and these can be classified into three categories - 1) the defrosting mechanism and scheme; 2) evaluation of the defrosting performance; 3) adaptive demand defrost.

On the defrosting mechanism and scheme, Aoki et al.[7-9] proposed the defrosting model for snow melting in a test box by heating from the bottom surface, and compared numerical results with experimental data by dividing entire defrosting process into three periods - the melting preparation period, the frost melting period, and the moisture removal period. Inaba et al.[10-12] proposed a method to remove frost with radiation heat from an infrared lamp to a vertical/parallel plate. On the evaluation of the defrosting performance, Sugawara et al.[13-16] investigated hot gas defrosting used in heat pumps and proposed a defrosting efficiency which takes into account the melting efficiency and the moisture removal period. On adaptive demand defrost, Allard et al.[17] proposed a refrigeration system which can maintain refrigerating efficiency by introducing the concept that defrost starts at the required time, and Knoop et al.[18] presented an adaptive demand defrost based on the fact that moisture enters the refrigerator only when the door is open.

Since defrosting is an unsteady, 2-phase heat transfer process and the shape of the actual heat exchanger is rather complicated, difficulties arise in conducting the theoretical and experimental investigations. Therefore, there are few studies on defrosting in the heat exchanger. Moreover, experimental data related to defrosting using electric heaters, which are commonly employed in refrigerators, are not available.

In this study, an experiment on frosting in a fin-tube heat exchanger and a defrosting experiment have been conducted to investigate the characteristics of defrosting for various conditions of frosting and defrosting.

2. Experiment

2.1 Experimental apparatus

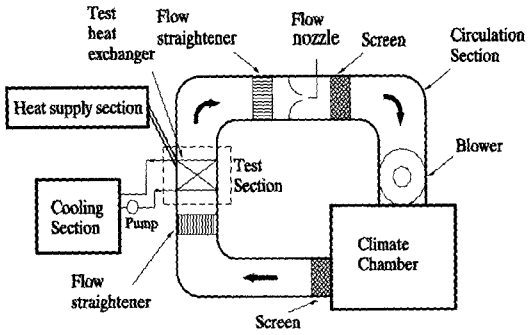

Fig.1 Schematic diagram of experimental apparatus.

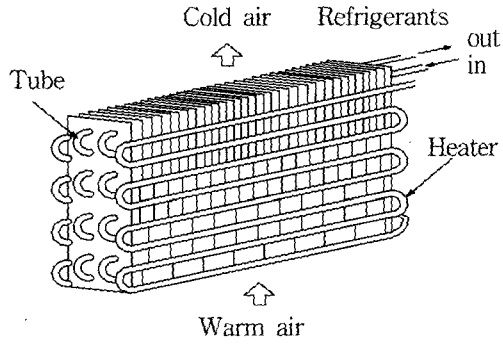

Fig.2 Fin-tube heat exchanger.

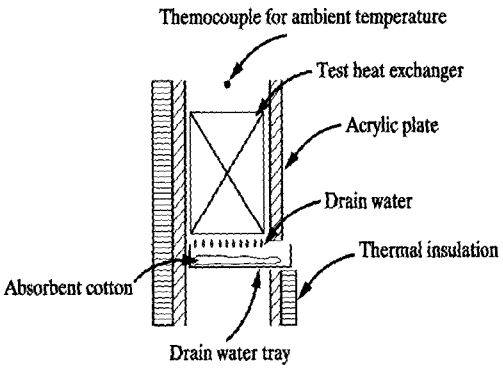

Fig.3 Side view of test section during the defrosting period.

Figure 1 shows a schematic diagram of the experimental apparatus. A fin-tube heat exchanger is installed in the test section to which a thermal insulator is attached to minimize heat loss. The front side of the test section is constructed from an acrylic resin plate to observe frosting and defrosting behavior. The temperature and humidity of the air induced into the test section are controlled by experimental conditions pre-determined by a climate chamber equipped with a refrigerator and a dry/wet bulb heater. The air flow rate brought into the test section is kept constant using an inverter installed in the fan, and a flow straightener is placed in front of the test section in order to make the air flow uniform. A solution of ethyleneglycol and distilled water is used as the refrigerant. The surface temperature of the heat exchanger is kept constant by circulating the refrigerant with a pump and the flow rate of the refrigerant is controlled by transforming the number of revolutions of the pump, operated by a signal fed back from the flowmeter. The electric power supplied to the electric heater is controlled by slidacs, and is measured by a digital wattmeter.

Figure 2 shows the fin-tube exchanger installed inside the test section. There are two columns and eight rows of tubes in the heat exchanger, and the length of the tube, not including the curved section, is 400 mm. The pin pitches of each row of the heat exchanger are arranged as 20, 10, 10, 7, 7, 5, 5, 5 mm, respectively, from the bottom row. An electric heater is connected to the fins staggered between the tubes. To measure the temperature of the fin, tube and heater in the heat exchanger during the defrosting period, type-T thermocouples(φ 0.1 mm) are placed at the center of the upper, middle, and lower sections of the heat exchanger.

2.2 Experimental method

First, the inlet air is induced into the test section at a fixed velocity, and the circulating

air temperature and humidity are also controlled. At the same time, the refrigerant in the brine tank is cooled to a pre-determined temperature. After the inlet air temperature and the refrigerant temperature reach their preset values, the frosting experiment starts by circulating the refrigerant through the heat exchanger. When the frosting experiment is done, the defrosting experiment starts by stopping the air flow into the circulation section and turning on the defrosting heater. At this time, sheets of tissue, which are weighed in advance, are laid on a drain water tray placed on the lower part of the test section to measure the amount of draining water as shown in Fig.3. The tray is exchanged at fixed time intervals, and the amount of the water drained is calculated by subtracting the initial weight of the tissues from the total weight. The tissues are measured with a digital chemical balance, and they are replaced at every exchange. When the tube surface temperature of the central location of the upper section of the heat exchanger reaches 14℃, the heat supply from the electric heater is suspended. After a certain resting(layoff) period, the defrosting experiment ends. Finally, the amount of residual water which remains on the fin and tube surfaces are measured.

To investigate the defrosting performance of the heat exchanger, we define melting and defrosting efficiencies as follows:

$$\eta_m = \frac{m_f L}{q_{heater}\tau_m} \tag{1}$$

$$\eta_d = \frac{m_f L}{q_{heater}\tau_d} \tag{2}$$

The uncertainties of the data in the amount of frost, the supplied power, and the melting and defrosting efficiencies are ±6.85%, ±1.8%, and ±7.08%, respectively.

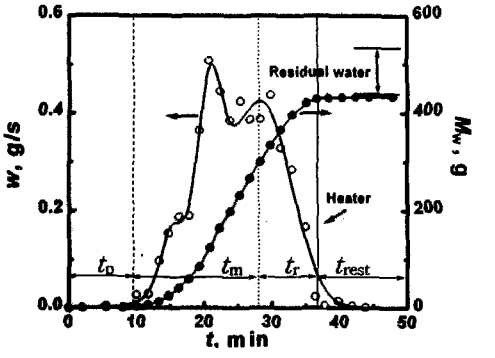

Fig.4 Water draining rate and total amount weight of draining water with defrosting time.

3. Experimental results and discussions

The standard experimental conditions for frosting are as follows: inlet air temperature of 6℃, relative humidity of 70%, and initial inlet air velocity of 1.35 m/s. The frosting experiment continues for 3 hours. The standard heat supply for defrosting is 167 W. When the tube surface temperature of the central location of the upper section of the heat exchanger reaches 14℃, the defrosting experiment ends. To investigate the influence of frosting conditions on the defrosting behavior, the experimental parameters are varied in such a way that inlet air humidity is varied from 50 to 86%, and the initial inlet air velocity from 1.35 to 2.0 m/s. The power supply of heater is also varied from 70 to 220 W.

3.1 General characteristics of defrosting

General characteristics of defrosting can be deduced from the temperature variation of each component and the corresponding behavior of the draining water. Fig.4 shows the time history of water draining rate and the total amount of

draining water. The time when the draining water is first discharged from the heat exchanger is about 7 minutes after the heat is supplied to the electric heater and the amount is very small. The draining rate gradually increases with time, and the first local maximum value appears at about $t=20$ min. After that it shows rather oscillating pattern and appears the last local maximum appears at about $t=28$ min. Thereafter, the draining rate decreases drastically. The defrosting ends at $t=37.2$ min when the surface temperature of the tube reaches 14 ℃ and the power supplied to the heater is suspended. According to such behavior of the draining water, the total amount of draining water increases noticeably between $t=10$ min and the defrost ending time. However, only a trace of melting water drains out after the power supply is suspended.

A noticeable characteristic of the draining water shown in Fig.4 is that there exist several local maxima in the water draining rate. To analyze this phenomenon, it is necessary to understand the frost melting mechanism. The frost on the heat exchanger is a porous medium and thus melting water does not drain instantaneously but permeate through the inside of the frost by capillarity when heat from the heater is supplied. When the water inside the frost becomes saturated, it starts to drain. Theoretically, the distribution of the water draining rate over time should have a smoothly curved shape. In reality however, there are several local maxima because the frost, on the fin-tubes, drops(by gravity) before it is fully saturated with the permeated water and it is added to the total amount of draining water with pure melting water. The first local maximum shows the maximum draining rate because a large amount of frost is drained along with melting water as discussed above. These phenomena are observable by the naked eye. At the final local maximum at t=28 min, only pure melting water has drained.

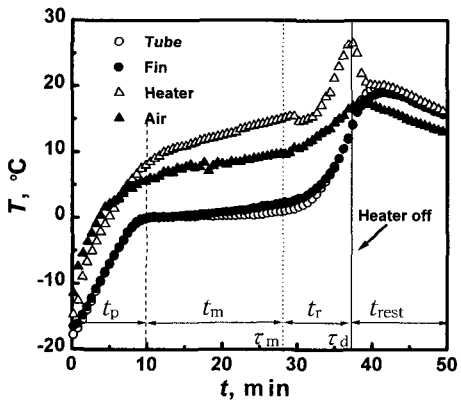

Fig.5 The variation of temperature in test section with defrosting time.

From the characteristics of the surface temperature of the fin-tube of the heat exchanger as shown in Fig.5, the defrosting process can be divided into four periods: the melting preparation period(t_p); the frost melting period(t_m); the moisture removal period(t_r); and the rest period(t_{rest}). During the melting preparation period, the temperature of the fin-tube rises to 0 ℃, and it lasts for about 27 % of the defrosting time(τ_d), up to $t=10$ min after the starting of defrosting. Heat supplied in this period is consumed to raise the frost temperature. The frost melting period is when the temperature of the fin-tube remains constant at 0℃ and the frost starts to melt, up to $t=28$ min, which takes about 48 % of defrosting time. During the moisture removal period, the temperature of the fin-tube rises to the defrost ending temperature of 14 ℃ at $t=37.2$ min, and takes about 25 % of the defrosting time. In this period, completely melted frost is discharged as drain water. The rest period is when the residual water completely drains out for 13 minutes after the heat supplied from the heater is suspended. In this

period, only 0.4% of the total amount of the frost deposited is discharged.

Here, the frost melting period may be regarded as the actual defrosting period. Starting from this period, the frost on the fin-tube starts to melt, and frost and melting water coexist. During this period, over 75% of the melting water has drained, not including the residual water, and it consumes about 48% of the power supplied. Most of the local maxima of the water draining rate also exist during this period. About 10 min after the beginning of the frost melting period, the first local maximum of the water draining rate appears and it shows a maximum amount of the frost melting discharged. Right after the end of the period, i. e., at about $t=28$ min, the last local maximum of the water draining rate appears.

Variations of air temperature in the test section and of temperature of the heater are also shown in Fig.5. The heater temperature was initially −15℃, however it rises faster than that of the fin-tube. Moreover, the temperature rises continuously without a period held at 0℃ because the frost on the heater melts very fast by heat transferred from the heater. Major portion of the drain water at the early stage is due to the frost on the heater. Initial air temperature in the test section is about −11℃, somewhat higher than that of the other components, when defrosting starts. During the melting preparation period, the temperature rises abruptly but during the frost melting period it stays constant like the fin-tube temperature. This results from the fact that heat loss to the surrounding air decreases as the heat from the heater is consumed to melt the frost deposited on the fin-tube. During the moisture removal period, the heat from the heater increases the heat transfer to the surrounding air by convection. Hence, the air temperature continues to rise, finally reaching that of the fin-tube at the end of defrosting period.

3.2 The effects of operating parameters on the frosting

Figure 6 shows the melting time(τ_m) and the ratio of the frost melting period(t_m) to defrosting time(τ_d) as a function of the amount

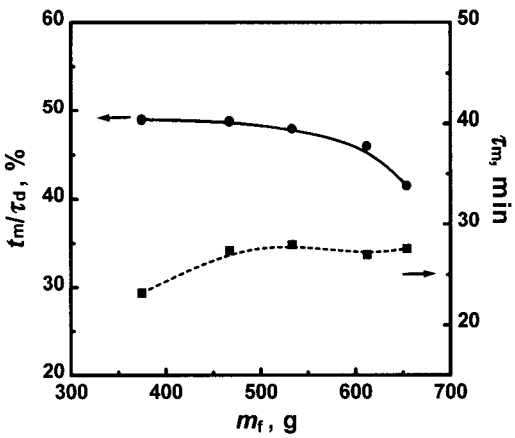

Fig .6 The ratio of frost melting period and melting time with the weight of frost for relative humidity.

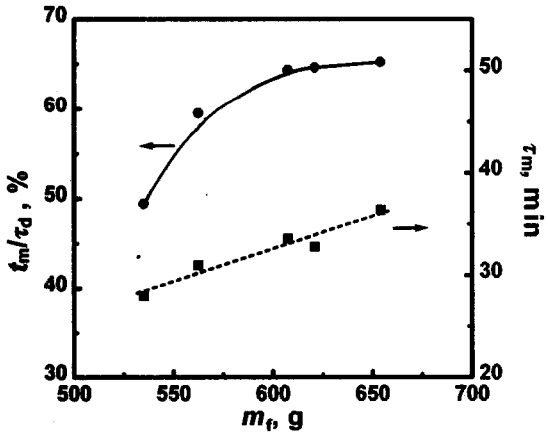

Fig.7 The ratio of frost melting period and melting time with the weight of frost for air velocity.

of frost with varying inlet relative humidity. The melting time becomes constant over a certain amount of frost. It may be attributed to the fact that the frost melting velocity becomes faster due to the easy permeation of the melting water through the frost layer, since frost with a relatively low density forms on the fin-tube when the relative humidity is high. Therefore, the ratio of the frost melting period to defrosting time decreases because the frost melting time does not increase as much as the amount of frost.

Figure 7 shows the melting time and the ratio of the frost melting period to defrosting time as a function of the weight of frost for various air velocities. The melting time increases linearly with the weight of frost. This differs from the case of controlling the inlet air humidity and is due to the fact that the frost with relatively high density forms as the inlet air velocity is increased and thus it is difficult to melt the frost. Therefore the ratio of the frost melting period to defrosting time increases with the weight of the frost. However, the rate slows over a certain amount of frost because the defrosting time increases with an increasing ratio of frost melting time at some point.

Figure 8 shows the melting(η_m) and defrosting(η_d) efficiencies, and residual water weight with the weight of frost for various relative humidities of the inlet air. Both melting and defrosting efficiencies increase linearly with the weight of frost. This results from the fact that the ratio of melting time decreases because the density of frost becomes relatively low, resulting in a fast frost melting velocity. However, the amount of residual water on the heat exchanger remains constant, irrespective of the amount of frost due to the influence of surface tension which represents the individual characteristics of the heat exchanger.

Figure 9 shows the melting and defrosting efficiencies as a function of the amount of frost with varying inlet air velocity. The melting and defrosting efficiencies increase linearly but their slopes are small compared to those with varying inlet air humidity. This results from the fact that the melting time increases linearly as explained above. The efficiency marginally improves because the duration of the melting and defrosting periods do not increase as much as the frost does. Therefore, the defrosting efficie-

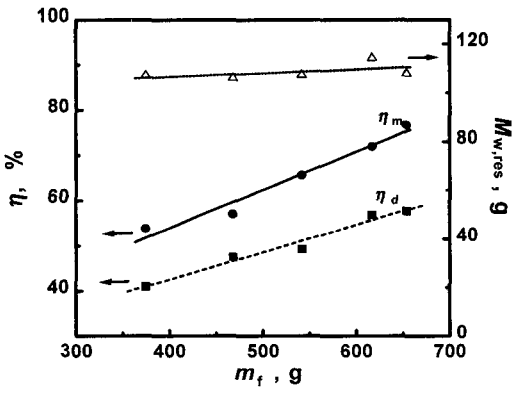

Fig.8 Melting and defrosting efficiencies and residual water weight with the weight of frost for relative humidity.

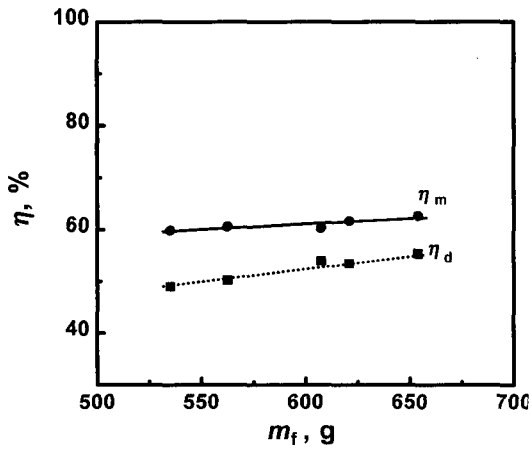

Fig.9 Melting and defrosting efficiencies with the weight of frost for air velocity.

ncy will increase when defrosting starts with a largeamount of frost, irrespective of the frosting condition, if one considers only the effectiveness of the defrosting without taking into consideration the degradation of the thermal performance due to the frosting as shown in Figs. 8 and 9.

In Fig.10 the defrosting behavior in the case of controlled inlet air humidity(1.35 m/s, 78%) is compared with that of the case of controlled initial inlet air velocity(1.8 m/s, 70%) when a similar amount of frost forms. The draining of melting water takes place earlier when the air velocity is controlled, but the local maximum point of the draining rate of the melting water shows rather similar behavior. The defrosting time increases somewhat and the curve of the water draining rate shows a wider distribution with a small value. This may be attributed to the fact that the melting water drains away continuously because the melting velocity of the frost becomes slow, even if the draining of melting water occurs earlier than the frost with a low density. This is due to the difficulties of the permeation of melting water through the frost layer since the frost with a relatively high density forms on the fin-tube when controlling the initial inlet air velocity.

3.3 The influence of supplying power for defrosting

Figure 11 shows how the water draining rate varies with the supplied power under standard conditions for frosting. When the supplied power is less than the standard value of 167 W, the curve of the draining rate of melting water shows a moderate slope during the defrosting period, and a considerably large amount of melting water is drained during the rest period. Moreover, when the supplied poweris 70 W, the defrosting time increases by 44% compared to that of the standard heat input. When the heat input is large, the defrosting time becomes shorter, the maximum water draining rate becomes higher, and there is little water draining during the rest period. The reason why the maximum water draining rate becomes higher with higher heat input is due to the fact that the defrosting time becomes shorter due to faster melting of the frost during the early period of defrosting, and a large amount of frost, which is not sufficiently permeated by the melting water, is drained.

Figure 12 shows the variation of air temperature inside the test section with a varying su-

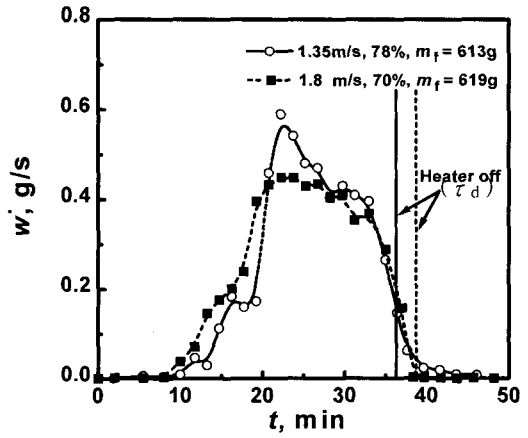

Fig.10 Water draining rate with defrosting time.

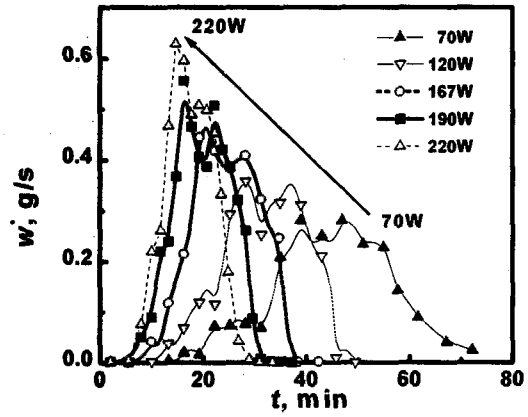

Fig.11 Water draining rate with defrosting time for supplying power.

pply of power. In an actual refrigeration system, the temperature of the air around the heat exchanger during the defrosting period increases a lot, causing the degradation of the thermal performance of the refrigerating and freezing equipment. As shown in the figure, the higher the supply of power, the shorter the melting time, however the surrounding air experiences a relatively high temperature increase. This results from the increasing heat loss to the surrounding air with a higher supply of power.

Shown in Fig.13 are the melting anddefrosting efficiencies with varying power supplies. When the power supply is less than 120 W, both melting and defrosting efficiencies are high at 100 % and 80 %, respectively, for 70 W. On the other hand, when the power supply is over 120 W, the melting and defrosting efficiencies are 65 % and 55 %, respectively. At a lower supply of power, the melting and defrosting efficiencies increase because of the reduction of the total supplied power, due to frost melting by permeation of melting water as well as lower heat loss to the surrounding air. In the case of high supplying power, both the melting and the defrosting efficiencies remain constant. This may be attributed to the fact that the total supplied power becomes similar due to the increasing heat loss to the surrounding air with the high supply of power, although a relatively large amount of unmelted frost is drained in this case.

4. Conclusions

In this study, experiments on the behavior of defrosting in a fin-tube heat exchanger have been conducted for various conditions of frosting and defrosting. The conclusions from the present work are as follows;

(1) Owing to a large amount of draining of the incompletely melted frost during the early stage of defrosting period, there are several local maxima in the water draining rate.

(2) The amount of residual water on the heat exchanger after the completion of the defrosting period remains constant, irrespective of the conditions of frosting and defrosting due to the influence of surface tension.

(3) The defrosting efficiency will be increased when defrosting starts with a large amount of frost, irrespective of the frosting condition, if

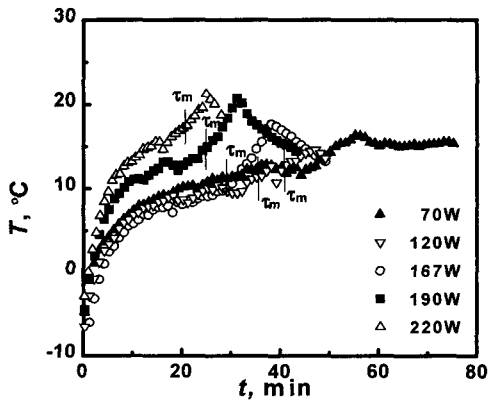

Fig.12 The variation of air temperature with defrosting time for supplying power.

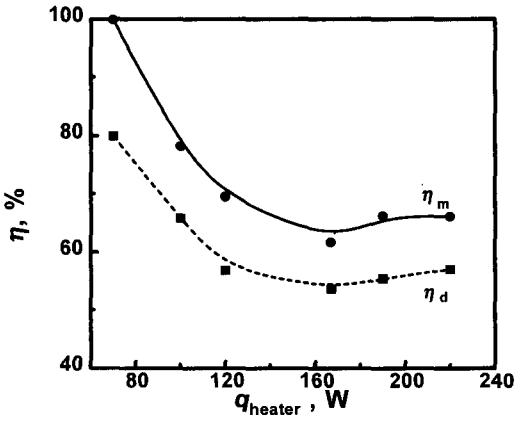

Fig.13 Melting and defrosting efficiencies with supplying power.

one considers only the effectiveness of the defrosting without taking into consideration the degradation of the thermal performance due to the frosting.

(4) It is also shown that the quantities such as melting / defrosting time, melting / defrosting efficiency, etc., vary with the experimental operating conditions during the frosting period, and the defrosting behavior is affected by the frost density as well as the amount of frost.

(5) With decreasing heat input, the heat loss to the surrounding air decreases, and the melting and defrosting efficiencies become high.

Acknowledgement

The authors wish to acknowledge the financial support of the Korea Research Foundation made in the program year of 1998(Grant No. 98-018-E00161/ME97-F-12).

References

(1) Lee, K. S., Lee, T. H., and Kim, W. S., 1994, "Heat and mass transfer of parallel plate heat exchanger under frosting condition", *Korean Journal of SAREK*, Vol. 6, No. 2, pp. 155-165.

(2) Lee, K. S., Lee, T. H., and Kim, W. S., 1995, "An experimental study on the effects of design factors for the performance of fin-tube heat exchanger under frosting condition", *Korean Journal of KSME*, Vol. 19, No. 10, pp. 2657-2666.

(3) Lee, K. S., Kim, W. S., and Lee, T. H., 1997, "A one dimensional model for frost formation on a cold flat surface", *Int. J. Heat Mass Transfer*, Vol. 40, No. 18, pp. 4359-4365.

(4) Jones, B. W. and Parker, J. D., 1975, "Frost formation with varying environmental parameters", *J. Heat Transfer*, Vol. 97, pp. 255-259.

(5) O'Neal, D. L. and Tree, D. R.,1984, "Measurement of frost growth and density in a parallel plate geometry", *ASHRAE Trans.*, Vol. 90, Pt. 2., pp. 278-290.

(6) Aoki, K., Hattori, M., and Edayoshi, A., 1989, "Characteristics on heat pump system due to frosting", *ASME*, Vol. 4.

(7) Aoki, K., Hattori, M., Chiba, S., and Hayashi, Y., 1981, "A study of the melting process in ice-air composite materials", *ASME* paper 81-WA/HT.

(8) Aoki, K., Hattori, M., and Chiba, S., 1986, "A study of the melting process in ice-air composite materials", *Bull. JSME*, vol. 29, No. 253, pp. 2138-2144.

(9) Aoki, K., Hattori, M., and Ujiie, T., 1988, "Snow melting by heating from the bottom surface", *JSME International Journal series II*, Vol. 31, No. 2, pp.269-275.

(10) Inaba, H., Otake, H., and Nozu, S., 1992, "Fundamental study on a horizontal frost layer melted from above by radiative heat", *JSME(B)*, 58-555.

(11) Inaba, H. and Otake, H., 1993, "Snow melting mechanism of radiative heat absorption material", *JSME(B)*, 59-567, pp. 278-285.

(12) Inaba, H. and Imai, S., 1996, "Study on sublimation phenomenon of horizontal frost layer exposed to forced convection air flow and radiation heat", *Transactions of the ASME*, Vol. 118 pp. 694-701.

(13) Sugawara, M., Kirihoshi, C., and Fujita, T., 1988, "The melting behavior of an ice particles layer on a heated base with fins, *JSME(B)*, 54-508, pp. 2838-2841.

(14) Sugawara, M., Uemura, S., Yajima, R., Kirikoshi, C., and Fujita, T., 1989, "Study

of melting of frost on heat exchanger for heat pump", *JSME(B)*, 55-510, pp. 504-509.

(15) Sugawara, M., Uemura, S., Yajima, R., Takahashi, T., and Fujita, T., 1990, "Melting of frost on heat exchanger of a heat pump", *JSME(B)*, 56-531, pp. 3457-3461.

(16) Sugawara, M., Sakae, S., and Fujita, T., 1991, "A basic study of defrost of heat exchanger", *JSME(B)*, 57-537, pp. 1874-1879.

(17) Allard, J. and Heinzen, R., 1988, "Adaptic defrost", *IEEE Transactions on Industry Applications*, Vol. 24, No. 1, pp. 39-42.

(18) Knoop, D. E., Tershak, A. T., and Thieneman, M., 1988, "An adaptic demand defrost and two-zone control and monitor system for refrigeration products", *IEEE Transactions on Industry Applications*, Vol. 24, No. 2, pp. 337-342.

이 논문집은 한국과학기술단체 총연합회의 일부 재정지원에 의하여 발간되었슴